Linear Bounds on an Uncertain Non-Linear Oscillator: An Info-Gap Approach

Yakov Ben-Haim[1] and Scott Cogan[2]

Abstract

We study a 1-dimensional cubic non-linear oscillator in the frequency domain, in which the non-linearity is roughly estimated but highly uncertain. The task is to choose a suite of linear computational models at different excitation frequencies whose responses are useful approximations to, or upper bounds of, the real non-linear system. These model predictions must be robust to uncertainty in the non-linearity. A worst case for the uncertain non-linearity is not known. The central question in this paper is: how to choose the linear computational models when the magnitude of error of the estimated non-linearity is unknown. A resolution is proposed, based on the robustness function of info-gap decision theory. We also prove that the non-probabilistic info-gap robustness is a proxy for the probability of success.

1 Introduction

Structural reliability is an important concern for high consequence engineering systems and many qualitative and quantitative arguments come into play in certifying a design for an intended application. For example, component-level qualification tests as well as numerical simulations integrating component models into global structural analyses are an integral part of the certification process for aerospace structures and subassemblies. However, the dominant sources and degrees of lack-of-knowledge in the studied system and its environment are often difficult to characterize and it is clearly desirable that design decisions be as robust as possible to these uncertain quantities. In particular, non-linearities may be present in material behavior and joint properties, due to a wide variety of spatial and time-dependent phenomena (e.g. plastic strain, stick-slip, impact, aging, . . .) and can modify the structural behavior in dramatic and often unsuspected ways. The importance of these effects is often observed during qualification tests at multiple excitation levels. While deterministic nonlinear dynamic analyses on complex global assemblies are not uncommon today, the computational burden of such computations is evidently much higher than for linear systems.

---

[1]Yitzhak Moda'i Chair in Technology and Economics, Faculty of Mechanical Engineering, Technion—Israel Institute of Technology, Haifa, Israel, yakov@technion.ac.il

[2]FEMTO-ST Institute, Université de Franche-Comté, Besançon France, scott.cogan@univ-fcomte.fr

In what follows, we propose a methodology that addresses both of these challenges—lack-of-knowledge and computational burden—by selecting a suite of linear computational models that approximates the upper bound of the real non-linear system given uncertainty in non-linear stiffness properties. Moreover, we assume that a worst case for this uncertainty is not known. A method is proposed based on the info-gap robustness function, that allows the trade-offs between robustness and linear model design to be studied over a range of behaviors. The proposed methodology is illustrated on a single degree of freedom oscillator with an uncertain cubic stiffness term. A frequency domain approach is adopted here and the excitation is assumed to be periodic. The non-linear responses are approximated using a first-order harmonic balance technique which assumes that the system responds at the excitation frequency.

Info-gap theory [1, 2] has been used in a wide range of engineering analysis problems. Matsuda and Kanno [7] study the info-gap robustness of structures based on plastic limit analysis with uncertain loads. Kanno and Takewaki [5, 6] study the robust design of structures under load uncertainty. Duncan *et al.* [4] develop an info-gap approach to robust decision making under severe uncertainty in life cycle design. Vinot *et al.* [9] develop a robust model-based test planning procedure. Pierce *et al.* [8] employ an info-gap technique to assess reliability of neural network-based damage detection.

2   Dynamics, Uncertainty and Robustness

In this section we formulate the info-gap robustness function, which is a combination of 3 elements: system models, a performance requirement, and an uncertainty model.

We consider two models in the time and frequency domains: the real non-linear system and an artificial computational model.

Real system. The equation of motion in the time domain is expressed as:

$$f = k_1 x + j b \dot{x}_r + m \ddot{x}_r + k_3 x_r^3 \tag{1}$$

where b and m are assumed known, but k_1, k_3 and f may be uncertain.

The response of this system will be calculated using the harmonic balance technique where the external excitation is assumed to be monoharmonic [10], $f = F \sin(\omega t + \phi)$ with phase angle ϕ, and the amplitude of response is periodic, $x_r = X_r \sin \omega t$. Balancing sine and cosine terms, and using the trigonometric equality $\sin^3 a = \frac{3}{4} \sin a - \frac{1}{4} \sin 3a$, yields:

$$-m\omega^2 X_r + k_1 X_r + \frac{3}{4} k_3 X_r^3 = F \cos \phi \tag{2}$$

$$b\omega X_r = -F \sin \phi \tag{3}$$

where the term in $\sin(3\omega t)$ has been neglected. Eliminating ϕ leads to the

following polynomial equation in X_r as a function of ω:

$$\left(\left(-m\omega^2 + k_1 + \frac{3}{4}k_3 X_r^2 \right)^2 + (b\omega)^2 \right) X_r^2 - F^2 = 0 \qquad (4)$$

The physically meaningful solutions of this equation correspond to the strictly real and positive roots. The solutions used in the computations that follow correspond to the upper portion of the non-linear frequency response function (between points A and B) as seen in fig. 1.
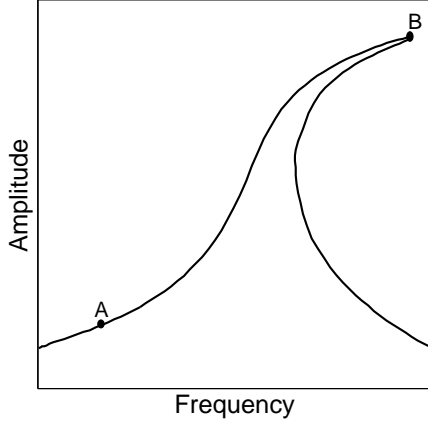

Figure 1: Non-linear frequency response function with cubic stiffness.

Computational model. The equation of motion in the time domain is given by:

$$F \cos \omega t = k_c x + j b_c \dot{x}_c + m \ddot{x}_c + F_c \cos \omega t \qquad (5)$$

and its transformation in the frequency domain by:

$$F = (k_c + j\omega b_c - \omega^2 m)X_c + F_c \qquad (6)$$

where m is the same as in eq.(4). We are free to choose the stiffness k_c, damping b_c, and the auxiliary force F_c. The dimensionless damping factor is $\zeta_c = b_c/(2\sqrt{k_c m})$, which will typically be small, around 0.01.

Performance requirement. At specified load, F, and driving frequency, ω, the amplitude of the response of the computational model, X_c, must be an upper bound of the amplitude of the response of the real system X_r. Specifically, eqs.(4) and (6) in general have complex roots. Let $|X_c|$ denote the magnitude of the greatest real or complex root of eq.(6). Let $|X_r|$ denote the greatest positive and purely real (not complex) root of eq.(4), evaluated with the method of harmonic balancing. The performance requirement is:

$$|X_c| - |X_r| \geq \delta \qquad (7)$$

δ is the greatest allowed error in the bound. If $\delta \geq 0$ then $|X_c|$ must bound $|X_r|$ from above, with an excess no less than δ. For instance, when $\delta = 0$, then $|X_c|$ must be no less than $|X_r|$. If $\delta < 0$ then $|X_c|$ may be less than $|X_r|$, but by no more than δ.

This performance requirement may at first appear insufficient to determine the computational model. One might be inclined to choose k_c, b_c and F_c in the computational model so that $|X_c|$ will be very large. But how large? We don't know how wrong our estimate of the non-linearity is, so we don't know how large $|X_r|$ could be; it might exceed even a very large value of $|X_c|$. On the other hand, if $|X_c|$ is vastly greater than $|X_r|$ then the computational bound is useless. The resolution of this indeterminacy is obtained from the robustness function, as we will see.

Uncertainty model. We consider uncertainty in the linear and cubic stiffness coefficients of the real model, k_1 and k_3. We also consider uncertainty in the load amplitude, F. Let $\widetilde{k}_1$, $\widetilde{k}_3$ and $\widetilde{F}$ denote best estimates of these quantities ($\widetilde{F}$ may vary with frequency). Each of these quantities, $\widetilde{k}_1$, $\widetilde{k}_3$ and $\widetilde{F}$, is a known but perhaps unreliable estimate of the corresponding coefficient. We do not know by how much the estimate in fact errs. Let s_1, s_3 and s_F denote estimated errors of $\widetilde{k}_1$, $\widetilde{k}_3$ and $\widetilde{F}$. These error estimates do not constitute knowledge of a worst case. Rather, they reflect some information about the relative errors among the parameters. For instance, k_1 may be known more reliably than k_3, in which case $s_1 < s_3$. The absolute errors are unknown and unbounded. In some situations we may know the value one of the quantities with confidence, in which case its s-value is zero.

We use a fractional-error info-gap model [2] to represent these uncertainties:

$$\mathcal{U}(h) = \left\{ k_1, k_3, F : \left| \frac{k_1 - \widetilde{k}_1}{s_1} \right| \leq h, \left| \frac{k_3 - \widetilde{k}_3}{s_3} \right| \leq h, \left| \frac{F - \widetilde{F}}{s_F} \right| \leq h \right\}, \quad h \geq 0 \tag{8}$$

Each of the 3 inequalities can be understood as a fractional error. For instance, considering the cubic coefficient, the inequality states that the fractional error of the estimate, $\left| \frac{k_3 - \widetilde{k}_3}{s_3} \right|$, is bounded by the horizon of uncertainty, h. Each of the 3 fractional errors is dimensionless, and thus commensurable in terms of the horizon of uncertainty h. Since we do not know the magnitude of error—no realistic worst case is known—the horizon of uncertainty is unbounded. Thus $h \geq 0$. When $h = 0$ then each estimate is correct: there is no uncertainty. The uncertainty set $\mathcal{U}(h)$ becomes more inclusive as h increases. The info-gap model is an unbounded family of nested sets of possible realizations of k_1, k_3 and F.

Robustness function. We now define the robustness of the linear computational model, eq.(6), to uncertainty in the load amplitude and in the linear and non-linear stiffnesses of the real oscillator, eq.(4). The robustness is the greatest horizon of uncertainty, h, up to which the performance

requirement is satisfied for all realizations of the uncertain quantities:

$$\widehat{h} = \max \left\{ h : \left(\min_{k_1, k_3, F \in \mathcal{U}(h)} (|X_c| - |X_r|) \right) \geq \delta \right\} \tag{9}$$

This robustness function depends on the driving frequency and the nominal force, ω and $\widetilde{F}$, applied to the non-linear system. It also depends on the design parameters of the linear computational model, F_c, k_c and b_c.

3   Example: Uncertain Cubic Non-Linearity

In this section we illustrate the selection of a suite of linear computational models for robustly evaluating the upper bound of the response of an oscillator with an uncertain cubic non-linearity. We will consider multiple uncertainties in section 4. We assume that the other terms in the real model are known reliably. The known parameters are $k_1 = 0.3$, $m = 1$, and $F = 1$. We consider various driving frequencies ω. The estimated cubic coefficient is $\widetilde{k}_3 = 0.02$ and its estimated error is $s_3 = 0.1$. The dimensionless damping coefficient of the computational model is $\zeta_c = 0.01$.
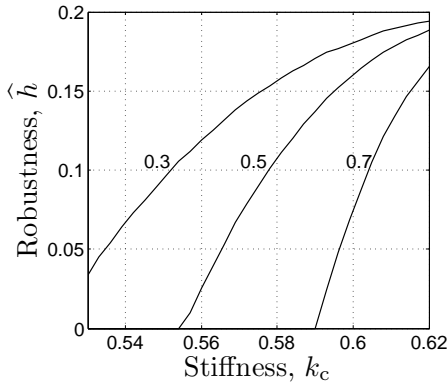

Figure 2: Robustness vs stiffness k_c of linear computational model, for 3 values of F_c: 0.3, 0.5 and 0.7. $\delta = 0$, $\omega = 0.8$.
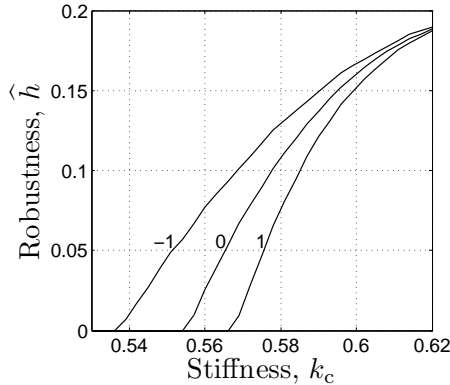
Figure 3: Robustness vs stiffness k_c of linear computational model, for 3 values of δ: -1, 0 and 1. $F_c = 0.5$, $\omega = 0.8$.

Figs. 2 and 3 display the robustness, $\widehat{h}$, vs. the stiffness, k_c, of the linear computational model.

Consider fig. 2, which shows robustness curves for three different values of the auxiliary load, F_c, of the linear model. At any level of robustness, $\widehat{h}$, the non-linear coefficient k_3 can deviate from its estimated value, $\widetilde{k}_3$, by as much as $\pm s_3 \widehat{h}$ around $\widetilde{k}_3$ without violating the performance requirement, eq.(7). Larger variation entails the possibility of violating the requirement. In this example $s_3 = 0.1$ and $\widetilde{k}_3 = 0.02$. Thus a robustness of 0.1 means that k_3 can

vary within ± 0.01 around 0.02 without violating the bound requirement. In other words, a robustness of 0.1 means that the estimated non-linear coefficient, $\widetilde{k}_3$, can err by as much as 50% and the linear computational model still provides an upper bound.

The driving frequency in fig. 2 is $\omega = 0.8$, so the linear system is at resonance if $k_c = 0.64$. This explains the positive slope of the curves. As k_c increases towards resonance, the value of X_c increases which allows the computational model to satisfy the upper bound requirement for a larger range of non-linearity. That is, the robustness increases as k_c moves towards resonance from lower values. The curve in fig. 2, if continued to higher k_c values, would display reflection symmetry around $k_c = 0.64$: the robustness would decline as k_c moves past resonance to higher values.

Fig. 3 shows robustness vs. k_c for three choices of the margin-of-error parameter, δ. The robustness increases as δ increases: allowing larger margin of error induces greater robustness. The absolute value of the maximal response of the non-linear system is in the range of 5 to 10 for robustness up to about 0.1. Thus a margin of error of 1 corresponds to about 10% or 20% of the non-linear response.
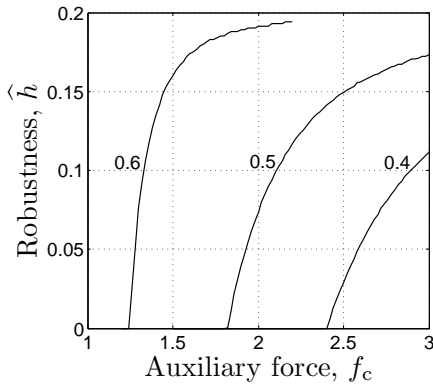

Figure 4: Robustness vs load F_c of linear computational model, for 3 values of k_c: 0.4, 0.5 and 0.6. $\delta = 0$, $\omega = 0.8$.
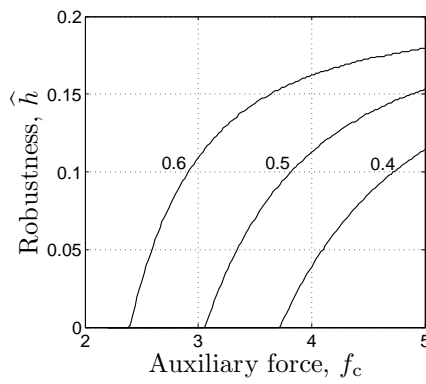
Figure 5: Robustness vs load F_c of linear computational model, for 3 values of k_c: 0.4, 0.5 and 0.6. $\delta = 0$, $\omega = 0.9$.

Figs. 4 and 5 show the robustness vs. the auxiliary load of the linear model, for several values of the stiffness of the linear model. These figures, if extended to lower F_c values, would both be reflection-symmetric around $F_c = 1$, which is the value of f. This is because the amplitude of X_c, in eq.(6) is determined by the magnitude, but not the sign, of $F - F_c$.

Next we note the monotonic increase of robustness with increase in F_c. Since the magnitude of $F - F_c$ increases as F_c increases over this range of values, we see that $|X_c|$ increases with increasing F_c. Thus the robustness increases monotonically over this range of F_c.

6

The decreasing positive slope of the robustness curves in figs. 4 and 5 results from the non-linearity. The magnitude of the non-linear response, $|X_r|$, increases as the value of the non-linear coefficient, k_3, gets smaller at $\omega = 0.8$. Thus the value of k_3 which produces the maximum non-linear response gets smaller as the horizon of uncertainty increases. Furthermore, the magnitude of the non-linear response increases more, for the same small change in k_3, when k_3 is small. Hence the increment of robustness, for each increment in F_c, decreases as F_c increases.

Finally, comparing figs. 4 and 5, we note that greater F_c is needed to achieve a given robustness at the larger driving frequency. This is because $\omega = 0.9$ is further above the resonance of the linear system than $\omega = 0.8$, so $|X_c|$ is smaller in the former case at fixed F_c.
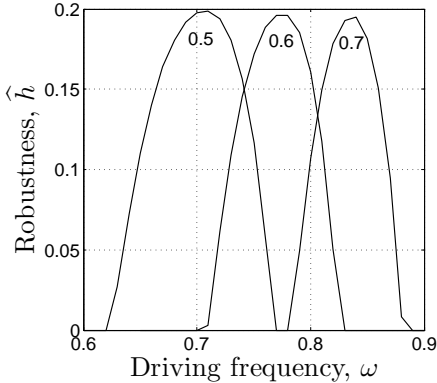

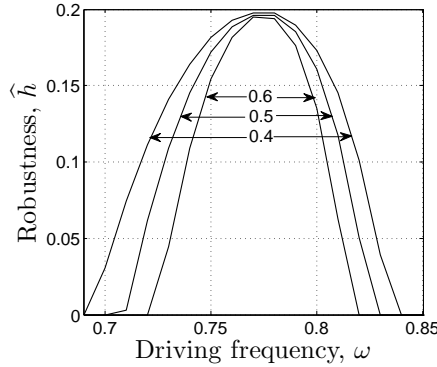Figure 6: Robustness vs driving frequency ω for 3 values of k_c: 0.5, 0.6 and 0.7. $F_c = 0.5$, $\delta = 0$.

Figure 7: Robustness vs driving frequency ω for 3 values of F_c: 0.4, 0.5 and 0.6. $k_c = 0.6$, $\delta = 0$.

Fig. 6 shows robustness, $\widehat{h}$, vs. driving frequency, ω, for several values of stiffness of the linear computational model, k_c. The figure shows that the robustness becomes small and vanishes ("detunes") rather quickly as the driving frequency changes. However, we see that k_c can be used to compensate for this by causing a shift in the ω-range with positive robustness.

Fig. 7 shows robustness, $\widehat{h}$, vs. driving frequency, ω, for several values of the auxiliary force, F_c. We again see the "detuning" of robustness. However, in contrast to fig. 6, F_c does not compensate, at least not very efficiently in this example.

Fig. 8 shows the robustness, $\widehat{h}$, vs. the margin of error for the upper bound, δ, for several combinations of k_c and F_c. The three solid curves show progressively greater robustness as F_c decreases, at fixed k_c. This is consistent with fig. 4 if we recall that the extension of that figure to values of F_c below 1 is the mirror image of the figure which is shown.

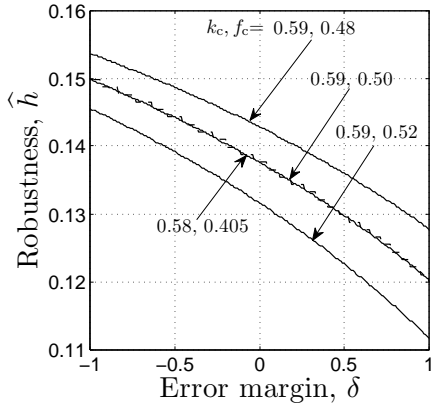Now notice the dashed curve in fig. 8, which very closely coincides with the

Figure 8: Robustness vs error margin δ, for several combinations of k_c and F_c. $\omega = 0.80$.
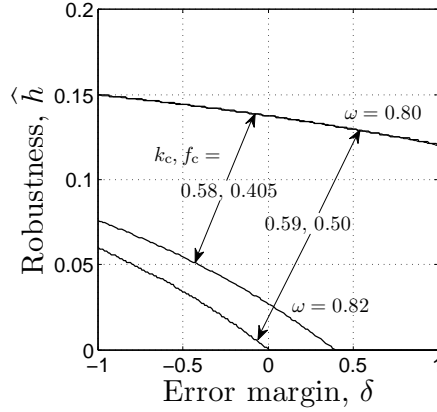
Figure 9: Robustness vs error margin δ, for several combinations of k_c and F_c. $\omega = 0.80$ and $\omega = 0.82$.

middle solid curve. This is for a slightly lower value of k_c and a substantially lower F_c. This demonstrates that k_c and F_c can compensate each other, resulting in distinct (k_c, F_c) pairs with essentially the same robustness to uncertainty.

Fig. 9 again shows robustness vs. error margin, at two different driving frequencies. The intermediate coinciding solid and dashed curves from fig. 6 are reproduced here, appearing in the upper part of fig. 9. The pair of curves in the lower part of fig. 9 are at the same values of k_c and F_c, but at a slightly larger driving frequency ω. We know from fig. 7 that the robustness can change dramatically with ω, which explains the strong separation of the curves at $\omega = 0.82$ while the same parameters cause closely coinciding curves at $\omega = 0.80$.

4 Example: Multiple Uncertainties

In this section we consider uncertainty in all three elements of the non-linear model, as specified in the info-gap model, eq.(8): k_1, k_3 and F. In all the calculations in this section we use $\widetilde{k}_1 = 0.3$, $\widetilde{k}_3 = 0.02$ and $\widetilde{F} = 1$. The estimated error of $\widetilde{k}_3$ is $s_3 = 0.1$, which is 5 times the value of $\widetilde{k}_3$. The estimated errors of $\widetilde{k}_1$ and $\widetilde{F}$, s_1 and s_F respectively, are either 0 or also 5 times the respective nominal values. The dimensional damping of the non-linear system is $b = 0.02$. The parameters of the linear computational model, when they are not varying on the horizontal axis, are $k_c = 0.5$ or 0.6, $F_c = 0.5$ and $\zeta_c = 0.01$. $\delta = 0$, $m = 1$ and $\omega = 0.8$ in this section.

The main conclusion we will draw is that uncertainty in the cubic stiffness coefficient, k_3, dominates the uncertainty in the linear stiffness, k_1, and the
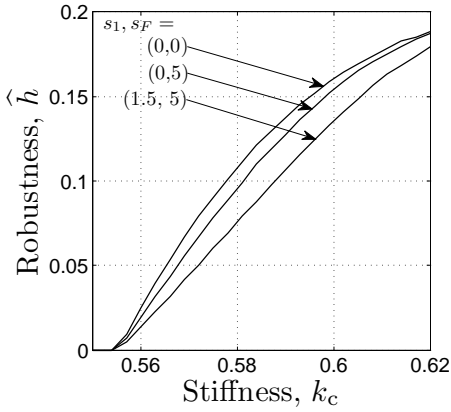
8

load, F.

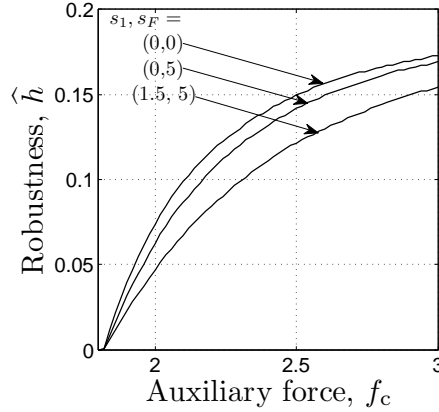Figure 10: Robustness vs stiffness k_c, for several combinations of s_1 and s_F.

Figure 11: Robustness vs auxiliary force F_c, for several combinations of s_1 and s_F. $k_c = 0.5$.

Fig. 10 shows robustness vs. the stiffness of the computational model, for different values of s_1 and s_F. These curves can be compared with the middle curve in fig. 2, which is actually the same as the upper curve in fig. 10. The most striking aspect of this figure is that introducing uncertainty in both k_1 and F (bottom curve) reduces the robustness by no more than about 15%. We also note that the drop in robustness from the top to the middle curve is less than the subsequent drop to the bottom curve. That is, uncertainty in the linear stiffness influences the robustness more than uncertainty in the load.

Fig. 11 shows robustness vs. auxiliary force, F_c, and should be compared with the middle curve in fig. 4 (which is the same as the upper curve in fig. 11). We again see that uncertainty in the load, F, reduces the robustness less than uncertainty in the linear stiffness k_1, and that together they reduce the robustness by less than 15%.

Fig. 12 shows robustness vs. driving frequency, ω, where the upper curve is the same as the middle curve in fig. 6. We see the same effect as in figs. 10 and 11.

Fig. 13 shows robustness vs. the error margin, δ, displaying the same small impact of uncertainty in k_1 and F, as compared to uncertainty in k_3.

5   Robustness as a Proxy for Probability

In this section we discuss a theorem which asserts that the non-probabilistic info-gap robustness is monotonically related to the probability that the non-
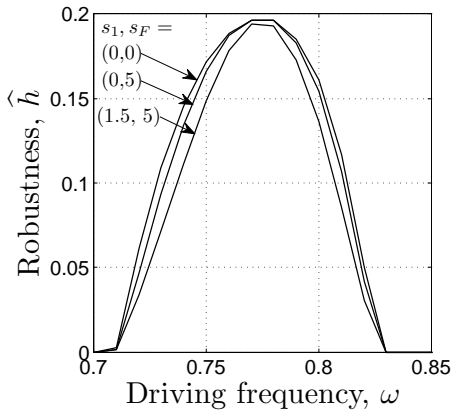
Figure 12: Robustness vs driving frequency ω, for several combinations of s_1 and s_F. $s_3 = 0.1$. $k_{\mathrm{c}} = 0.6$.
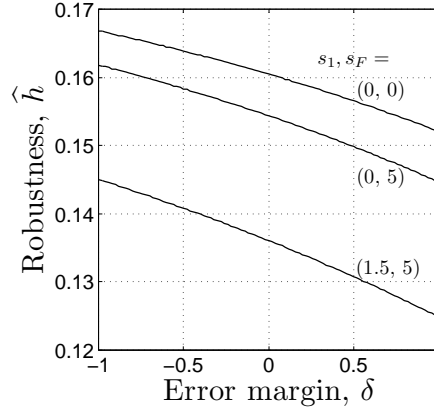
Figure 13: Robustness vs error margin, δ, for several combinations of s_1 and s_F. $s_3 = 0.1$. $k_{\mathrm{c}} = 0.6$.

linear system satisfies the performance requirement. This 'proxy property' is important since, when it holds, it implies that a computational model can be chosen which maximizes the probability of success, without knowing the probability distribution of the uncertain variables. The value of maximum probability will remain unknown. We begin with several definitions.

Let $q = (k_{\mathrm{c}}, b_{\mathrm{c}}, F_{\mathrm{c}})$ denote the design variables of the computational model, eq.(5). Note that the real system, eq.(1), does not depend on q. Likewise, let $c = (k_1, k_3, F)$ denote the uncertain parameters of the real system whose uncertainty is represented by an info-gap model such as eq.(8). Note that the computational model does not depend on c.

For any design, q, of the computational model, let $K(q)$ denote the set of all uncertain parameters c of the real system which satisfy the performance requirement in eq.(7):

$$K(q) = \{c: \ |X_{\mathrm{r}}(c)| \le |X_{\mathrm{c}}(q)| - \delta\} \tag{10}$$

We will suppose that a probability distribution exists for the parameters c of the real system, though this distribution is unknown. For any set, A, of coefficients c, let $P(A)$ denote probability of this set.

For any design, q, we define the probability of success as the probability that c takes a value which satisfies the performance requirement, eq.(7). Thus the probability of success of computational design q is the P-measure of the set $K(q)$:

$$P_{\mathrm{s}}(q) = P[K(q)] \tag{11}$$

All info-gap models, such as eq.(8), are **nested**, meaning that:

$$h < h' \implies \mathcal{U}(h) \subseteq \mathcal{U}(h') \tag{12}$$

10

Given an info-gap model, $\mathcal{U}(h)$, let $\widehat{h}(q)$ denote the robustness to uncertainty in the real system as defined in eq.(9), for any design, q, of the computational model.

We will say that **robustness is a proxy for the probability of success** if any change in the design of the computational model which enhances the robustness, does not reduce the probability of success. The following theorem asserts the proxy property for the system studied in this paper (see also lemma 1 in [3]).

Theorem. *Given the computational model, eq.(5), and the real system, eq.(1), whose uncertainty is represented by an info-gap model which is independent of q.* **If:**

$$\widehat{h}(q) > \widehat{h}(q') \tag{13}$$

then:

$$P_{\mathrm{s}}(q) \geq P_{\mathrm{s}}(q') \tag{14}$$

Proof. The proof derives from the following sequence of implications:

$$\widehat{h}(q) > \widehat{h}(q') \quad \Longleftrightarrow \quad |X_{\mathrm{c}}(q)| > |X_{\mathrm{c}}(q')| \tag{15}$$
$$\Longrightarrow \quad K(q) \supseteq K(q') \tag{16}$$
$$\Longrightarrow \quad P_{\mathrm{s}}(q) \geq P_{\mathrm{s}}(q') \tag{17}$$

Implication (14): Let us re-write the robustness in eq.(9) as:

$$\widehat{h} = \max \left\{ h : \left(\min_{c \in \mathcal{U}(h)} (-|X_{\mathrm{r}}(c)|) \right) \geq \delta - |X_{\mathrm{c}}(q)| \right\} \tag{18}$$

The info-gap model is nested, meaning that the sets $\mathcal{U}(h)$ become more inclusive as h increases. Thus the inner minimum in eq.(18) cannot increase as h increases. Also, $|X_{\mathrm{r}}(c)|$ and $\mathcal{U}(h)$ are independent of q and $|X_{\mathrm{c}}(q)|$ is independent of c. Thus a change in q which enhances robustness can occur if and only if $|X_{\mathrm{c}}(q)|$ has increased.

(15) implies (16): Any c in $K(q')$ satisfies $|X_{\mathrm{r}}(c)| \leq |X_{\mathrm{c}}(q')| - \delta$ which is less than $|X_{\mathrm{c}}(q)| - \delta$. Hence that c also belongs to $K(q)$.

(16) implies (17): from the definition of $P_{\mathrm{s}}(\cdot)$ in eq.(11) and since probability in non-decreasing on nested sets. ∎

6 Conclusion

We propose a methodology, based on info-gap theory, for designing a linear computational model to represent a non-linear model with uncertain linear and non-linear stiffnesses and uncertain load. It is assumed that a worst case for the uncertainties is not known. An info-gap robustness approach is used to study the tradeoffs between robustness and design. The proposed methodology is applied to a 1-dimensional non-linear oscillator which is analyzed in the frequency domain under periodic excitations. In practice, the

analyst much decide on the level of robustness required in a given application. A suite of frequency dependent linear models is then generated to provide useful upper bounds on the uncertain non-linear responses. We show that the non-probabilistic info-gap robustness function can be used to choose a computational linear model for which the probability of bounding the non-linear model is maximized, without knowing the probability distribution of the parameters of the non-linear model.

Acknowledgement

References

1. Yakov Ben-Haim, 2005, Info-gap Decision Theory For Engineering Design. Or: Why 'Good' is Preferable to 'Best', appearing as chapter 11 in *Engineering Design Reliability Handbook,* Edited by Efstratios Nikolaidis, Dan M.Ghiocel and Surendra Singhal, CRC Press, Boca Raton.

2. Yakov Ben-Haim, 2006, *Info-gap Decision Theory: Decisions Under Severe Uncertainty,* 2nd edition, Academic Press, London.

3. Yakov Ben-Haim, 2007, Info-gap robust-satisficing and the probability of survival, De Nederlandsche Bank Working Papers, #138.

4. Duncan, S.J., Bras, B. and Paredis, C.J.J., 2008, An approach to robust decision making under severe uncertainty in life cycle design, *Int. J. Sustainable Design,* Vol. 1, #1, pp.45–59.

5. Y. Kanno and I. Takewaki, 2006, Robustness analysis of trusses with separable load and structural uncertainties, *International Journal of Solids and Structures,* vol. 43, #9, pp.2646–2669.

6. Y. Kanno and I. Takewaki, 2006, Sequential semidefinite program for maximum robustness design of structures under load uncertainty, *Journal of Optimization Theory and Applications,* vol.130, #2, pp.265–287.

7. Matsuda, Y. and Y. Kanno, 2008, Robustness analysis of structures based on plastic limit analysis with uncertain loads, *Journal of Mechanics of Materials and Structures,* vol.3, pp.213–242.

8. S.G. Pierce, K. Worden and G. Manson, 2006, A novel information-gap technique to assess reliability of neural network-based damage detection, *Journal of Sound and Vibration,* 293: #1–2, pp.96–111.

9. P. Vinot, S. Cogan and V. Cipolla, 2005, A robust model-based test planning procedure, *Journal of Sound and Vibration,* vol. 288, #3, pp.571–585.

10. K. Worden, and G. R. Tomlinson, *Nonlinearity in structural dynamics: detection, identification and modeling*, 2001, IOP, Bristol.